Characterisation and pore structure analysis of mortar incorporating valorised rice husk ash

SINGH, A., SINGH, B. and MANGAT, P.S. <http://orcid.org/0000-0003-1736-8891>

Characterisation and pore structure analysis of mortar incorporating valorised rice husk ash

Author 1

- Arshdeep Singh, Assistant Professor
- Department of Civil Engineering, Punjab Engineering College, Chandigarh,160012,India

Author 2

- Bhupinder Singh, Ph.D.
- Department of Civil Engineering, Indian Institute of Technology Roorkee, Roorkee, Uttarakhand, 247667, India

Author 3

- P.S. Mangat, Ph.D.
- Centre for Infrastructure Management, Materials and Engineering Research Institute, Sheffield Hallam University, Sheffield S1 1WB, UK

Full contact details of corresponding author.

Arshdeep Singh,

Assistant Professor,

Department of Civil Engineering,

Punjab Engineering College, Chandigarh,160012, India.

E-mail: *singharsh004@gmail.com*

Abstract

Physical, chemical, and mineralogical characterisation of as-received Rice Husk Ash (RHA) samples sourced from four rice-growing regions (North, South, East, and West) of India is presented. Valorised RHA was obtained through controlled combustion at two temperature ranges (600^{o}C–700^{o}C and 650^{o}C–700^{o}C) of husks from the North in an industry set up. Valorisation efficacy has been tested through comparative characterisation of the valorised RHAs with the as-received RHAs from the four regions. Blending of 15% valorised RHA (in the beneficiated state) by weight of cement had no adverse effect on compressive strength even though water-binder ratio of the blended mortar had to be increased by 14% to achieve flow of the control cement mortar. Compared to the control cement mortar, porosity of the mortar blended with the beneficiated RHA measured using Mercury Intrusion Porosimetry increased by up to 10% primarily due to an increase in the number of large mesopores (0.01-0.05 μm).

Keywords: Rice husk ash, Pozzolans, Reactivity, Supplementary Cementitious Material, Compressive strength.

1. Introduction

Estimated annual production of paddy in India is about 169 Million Tonnes (MT) (FAO RMM 2018) and its processing generates approximately one-fifth the weight of paddy as rice husks (Dizaji et al. 2019). It is also estimated that about one-fifth of the weight of these husks is converted into Rice Husk Ash (RHA) when for example rice husk is used as a fuel in energy co-generation processes (Singh 2018). Currently, most of this ash in the country is disposed off in landfills or simply dumped in the open. Due to combustion variabilities inherent in industries consuming rice husks as a fuel, significant scatter in the physical, chemical, and mineralogical properties of RHAs is reported in the literature (Dizaji et al. 2019; Zunino and Lopez 2017; Rêgo et al. 2015). In the context of combustion conditions, two studies report that residual carbon in RHA obtained from five to ten different industrial sources has been found to vary in the ranges 2%-24% (Zunino and Lopez 2017) and 2%-15% (Rêgo et al. 2015a). Since rice husk combustion conditions are reported to have the most significant influence on RHA properties, some of the optimum combustion temperature ranges reported in the literature based on small-scale pilot tests are 660^{o}C – 720^{o}C (Chen et al. 2015); 750^{o}C – 850^{o}C (Nehdi et al. 2003); 700^{o}C – 900^{o}C (Blissett et al. 2017) and 700^{o}C (Fernandes et al. 2016). Recommendations have also been made for airflow rates that result in the most optimum ash properties (Chen et al. 2015; Rozainee et al. 2008; Armesto et al. 2002). In addition, ash characteristics are also reported to be influenced by combustion technology (Fernandes et al. 2016; Zain et al. 2011), rate of heating (Chandrasekhar et al. 2006), and dwell time (Nair et al. 2006). For example, the optimum combustion temperature range for an expanded bed reactor is reported to be 700^{o}C – 900^{o}C (Blissett et al. 2017) whereas this range for a fluidised bed reactor is 660^{o}C – 720^{o}C (Chen et al. 2015). Considering the large number of parameters that can affect ash characteristics, significant variations in the quality of ash across different geographies of a vast country like India can be expected. This in turn can pose a challenge for the development of over-arching performance specifications for use of RHA as a supplementary cementitious material. The first step towards addressing this problem is characterization of ash from the representative geographies with the second step being investigation of ash valorisation options followed by testing the performance of ash as a Supplementary Cementitious Material (SCM). The target properties in a valorisation strategy can be taken from IS 269: 2015 (BIS 2015) which

inter alia requires an amorphous silica content of more than 80% and a residual carbon content < 5% for an acceptable SCM.

In this investigation, RHA samples of unknown combustion histories were collected from the North, East, South, and West regions of India respectively. Characterisation of these as-received ashes indicated the need for heat treatment since all of them had unburnt carbon >13%. In the literature, re-burning of ashes to remove excess unburnt carbon had been reported as a valorisation option (Ganesan et al. 2008; Mali and Nanthagopalan 2021), though this option will increase ash processing cost. In the valorisation exercise, control ashes of this study were produced by combusting at 2 temperature ranges locally available husks in the atmospheric fluidised bed boiler of an industrial partner, Kuantum Papers, located in the state of Punjab, India. Comparative characterisation of the four RHAs of unknown combustion history and the two control RHAs is reported together with those of three beneficiated ashes obtained through grinding (for varying intervals of time) of the 2 control ashes.

Some studies in the literature (Xu et al. 2012; Van et al. 2013) on RHA blended mortars and concretes report the use of RHA with an average particle size in the range of 0.15µm - 10µm. It is reckoned that this size range will require fine grinding of ash which may add to its processing cost. As an alternate and more practical option, in this investigation the role of beneficiated RHA as a SCM has been examined for a more realistic level of fineness defined as at least 66% of the sample passing through a 45µm sieve. This requirement corresponds to the minimum acceptable fineness limit for a Class N raw or calcined natural pozzolana in the ASTM C 618 (ASTM 2019). Notably, the relevant Indian Code, IS 269 (BIS 2015) has no recommendations for the minimum fineness of RHA proposed to be used as SCM.

In the limited studies in the literature (Gastaldini et al. 2009; Huang et al. 2017) pore size distribution in RHA blended mixtures has been reported in the form of comparison with plain cement mortar and concrete mixtures having the same water-binder ratios. It implies that super-plasticisers were used in the RHA blended mixtures for obtaining comparable flow behaviour. Chindaprasirt et al. 2007 noted that mortar blended with 20% RHA and containing extra water showed better compressive strength relative to the control mortar made with OPC as the only binder. No superplasticiser was used in this study to compensate for the potential loss of workability due to RHA since authors' attention was to investigate the effect of additional water

(up to maximum limit of 115% of control as per ASTM C 618) on the pore structure properties of valorised RHA blended mortars. Recommendations are made for optimum rice husk combustion conditions and desirable RHA physical, chemical and mineralogical characteristics. Guidelines are also given for optimum weight replacement of cement with RHA in blended mortars.

2. Materials and methods

2.1 Materials

Summary of the four as-received RHA samples of unknown combustion histories (R1, R2, R3, R4), two control RHAs (R5 and R6), and the beneficiated RHAs is presented in **Table S1**. Beneficiation of the control RHAs was carried out by grinding using a Los Angeles machine with a material-to-charge ratio of 1:3. The R5 sample was ground for 60 min, and 100 min. Based on the consistency and compressive strength results of the beneficiated R5 sample, the R6 sample was only ground for 100 minutes. In **Table S1**, the beneficiated R5 samples are identified as 'R5-G60', and 'R5-G100' and the R6 sample is identified as 'R6-G100'. Ordinary Portland Cement (OPC) of 43 Grade, having a specific gravity of 3.15 and conforming with IS 269 (BIS 2015) having Loss-On-Ignition (LOI) 2.19%, and standard sand conforming with IS 650 (BIS 1991) was used in the pastes and mortars which were tested as per relevant Indian standards.

2.2 RHA characterization

2.2.1 Chemical characterisation

Chemical composition of the RHA samples was evaluated using X-Ray Fluorescence (XRF) and is reported in **Table 1**. Loss-On-Ignition (LOI) test was performed in accordance with IS 1727 (BIS, 1967) to check the percentage of unburnt carbon.

2.2.2 Mineralogical characterisation

Mineralogical characterisation was carried out using X-Ray Diffraction (XRD). The RHA samples were analysed using Cu Kα radiation (λ=1.5402Å) and Co Kα radiation (λ=1.789Å) at an angle (2θ) range of 5^{o} to 100^{o} using a scanning rate of 0.013^{o}/s. An internal standard method was used to estimate total amorphous content in the RHA samples.

2.2.3 Physical characterisation

Physical characteristics in terms of fineness, specific gravity, surface area, and morphology were investigated in the as-received as well as in the other samples. Morphological studies were carried out using a scanning electron microscope. Brunauer–Emmett–Teller specific surface area (BET-SSA) was measured using a multi-point BET test and values were rounded off to the nearest ±0.5. The average particle size of the RHAs was examined using laser particle diffraction.

2.2.4 Pozzolanic reactivity

A volume replacement of cement with 20% RHA was done to measure the pozzolanic reactivity of RHA as per IS 1727 (BIS 1967). This test was performed on cement mortars. The percentage compressive strength of the blended cement mortar 50 mm size cubes with respect to the reference specimen (with cement as the only binder) was determined after 7 and 28-days of moist curing and used for calculation of pozzolanic reactivity. Samples R1, R2, R3, and R4 were investigated in the as-received state only. Flowability across all mortars was maintained in the range of 105 ± 5%.

2.3 Standard consistency

Standard consistency of the RHA blended cement pastes was determined in accordance with IS 4031 (Part 4) (BIS 1988) for 5%, 10%,15%, and 20% weight replacements of cement with the selected RHA. This test was carried out on the R5 sample (control and beneficiated) only. The quantity of water taken for each cube was (P/4+3) percent of the combined mass of binder and sand as recommended in IS 4031 (Part 6) (BIS 1988), where P is the percentage of water required to produce a paste of standard consistency.

2.4 Compressive strength

Amongst the control ashes, the R5 sample was tested as per relevant Indian standards and the R6 sample was tested as per ASTM standards. Compressive strengths of mortars blended with the R5 sample were investigated using 70.6 mm cubes in accordance with IS 4031 (Part 6) (BIS 1988). For each cube, 200 g of binder was mixed with 600 g of standard sand. The R5 sample

was tested in both the beneficiated and the unbeneficiated states and weight replacements of cement with RHA were 5%,10%,15%, and 20%.

Compressive strengths of the Plain Cement (PC) mortars (serving as the reference material) and the mortars blended with the beneficiated R6 sample (R6-G100) was tested in accordance with ASTM C 109 (ASTM 2020) for 10%,15%, and 20% weight replacements of cement with RHA. The binder-sand ratio was 1:2.75 and for each of the RHA replacement levels and water-binder ratio that produced 110 ± 5% flow of mortar was used. The mortar specimens were demoulded after 24 hrs and moist cured at 27 ± 2^{o}C until the test ages of 7- and 28-days. All the reported compressive strength results are the averages of three replicate samples. Qualitative microstructure analysis of the PC mortar and RHA (R6-G100) blended mortars was also performed using XRD, scanning electron microscopy (SEM) and Energy Dispersive X-Ray Analysis (EDX).

2.5 Mercury intrusion porosimetry

To investigate pore size distribution and total porosity, Mercury Intrusion Porosimetry (MIP) was performed on the PC and the mortars blended with the beneficiated RHA (R6-G100). The test samples were obtained from the mortar cubes cast for 28-day compressive strength testing. At least three pieces each approximately 6-8 mm square and 0.7-1g in weight were taken from the inner core of the cube specimens. First, these samples were placed inside an oven (100±5^{o}C) for 3 days to completely remove pore water and then placed inside a desiccator for 3 days. After this conditioning the samples were stored in a sealed plastic bag till testing. MIP was carried out on both blended and unblended mortars using a Pascal 140/240 Porosimeter which measures pore sizes in the range of 0.0073 to 100μm. The Washburn Equation, **(Eq. (1))** was used to relate applied pressure to pore diameter.

$$p = \frac{2y\cos\emptyset}{r} \quad (1)$$

where p is absolute applied pressure, r is pore radius, ϕ is the contact angle (=140^{o}), y is mercury surface tension (= 0.48 N/m).

3. Results and Discussion

3.1 RHA characterization

3.1.1 Chemical characterisation

As per **Table 1**, silicon dioxide (SiO_2) in R1, R2 & R4 is 61.3%, 70%, and 72.2% respectively. Only R3, R5, and R6 have SiO_2 contents that are equal to or more than 80%. The high LOI in R1 and R2 is associated with reduced silica content in these samples and the low silica content in R4 is attributed to both its high potassium oxide (K_2O) content and high residual carbon. In terms of percentage of SiO_2, the characteristics of the studied control RHA samples were found to be similar with the properties of RHAs of other Asian countries reported by (Zain et al. 2011; Xu et al. 2012; and Venkatanarayanan and Rangaraju 2013). However as observed in the studied RHA samples, a linear decreasing trend of SiO_2 content in RHA with increase in unburnt carbon was also reported by (Venkatanarayanan and Rangaraju 2013). SiO_2 content in RHA may also reduce in the presence of high K_2O (Bie et al. 2018). **Table 1** shows the chemical requirements of RHA samples which were compared with chemical requirements of ASTM C 618 (ASTM 2019) for Class N-raw or calcined natural pozzolanas, BS 8615-2 (BSI 2019) for high reactivity natural calcined pozzolana, and IS 269 (BIS 2015) for RHA. The 80% amorphous silica requirement of IS: 269 (BIS 2015) was not fulfilled by any of the RHA samples except for R6. However, the requirement of 70% combined oxides of silica, alumina, and ferrite (SAF) of ASTM C 618 (ASTM 2019) and BS 8615-2 (BSI 2019) was satisfied by all the RHAs except for R1. **Table 1** shows that none of the RHAs had unburnt carbon content below the 5% upper-bound limit of IS: 269 (BIS 2015) although for the control ashes (R5 and R6), LOI was within the upper-bound limit (10%) for Class N-raw or calcined natural pozzolans of ASTM C 618 (ASTM 2019). As per BS 8615-2 (BSI 2019) upper limit for unburnt carbon in natural calcined pozzolana is 7%.

3.1.2 Mineralogical Characterisation

Figure S1(a) presents the X-ray diffractograms (XRD) of R1, R2, R3, R4, R5, and R6. The R1 and R2 samples were found to be purely amorphous since no crystalline peak was noticed in their XRDs. Since residual carbon is also amorphous in nature, it may be responsible

for the high total amorphous content in these ashes (Batra et al. 2008). The presence of peaks in the R3 and R4 samples is indicative of the partially crystalline nature of these ashes. For a more objective analysis, the amorphous fraction in each sample was also evaluated using an internal standard method in which a precisely known quantity of an internal standard (i.e. pure silicon) was added to each RHA sample before XRD analysis followed by the Rietveld refinement of XRDs. As an illustration of such an analysis, XRDs of R5, and R6 obtained after the addition of standard silicon are presented in **Figures S1(b)** and **S1(c)** respectively. Analysis of these diffractograms indicates that in all the RHA samples the primary crystalline phases were cristobalite and quartz. In the R4, R5, and R6 samples, the total amorphous fraction (inclusive of all oxides) was more than 90% whereas the percentage of amorphous silica was 64%, 70%, and 80% respectively, **Table 1**. It may be noted that as per IS: 269 (BIS 2015) the minimum acceptable amorphous silica content in RHA is 80%. Another study, (Olalekan and Mangat 2018) reports reactive silica content of 70% -72% in Indian RHAs. (Zunino and Lopez 2017) concluded that RHA can be considered a promising pozzolanic material despite having substantial variation in the amorphous silica content which was 38% to 85%. As per BS 8615-2 (BSI 2019), amorphous silica in natural calcined pozzolanas should be more than 25% whereas no such limit is set by ASTM C 618 (ASTM, 2019). However, finely ground RHA having 17.66 % amorphous silica also showed adequate pozzolanic reactivity as studied by (Rêgo et al. 2015a). Hence, in the context of the BSI and ASTM requirements, R5 and R6 qualify as pozzolanic materials and the IS Code requirements seem to be overly restrictive.

Keeping this in mind, the authors are of the opinion that the replacement percentage of RHA should be decided in such a way that the total unburnt carbon of the binary binder (OPC+RHA) does not exceed the Indian Standard IS 269 (BIS 2015) specified maximum unburnt carbon limit of 5% for OPC. In this investigation, LOI of the cement and RHA (R6) was 2.19% and 7.3% respectively, and the maximum unburnt carbon in the binary blend of 80% OPC+20% control RHA (R6) was 3.21%.

3.1.3 Physical characterisation

3.1.3.1 Fineness

Measured physical properties are presented in **Table 1**. The wet sieve analysis results show that more than 80% of all the material in the as-received and in the control ashes was coarser than 45 µm which is neither in compliance with the fineness requirement for Class N-raw or calcined natural pozzolans in ASTM and BSI nor with any of the Indian Codes for pozzolanic materials. For example, IS 3812 (Part 1) (BIS 2013) specifies that in the case of fly ash not more than 34% of the particles should be retained on a 45 µm sieve. The specific gravity of the RHAs was found to be higher in the control ashes when compared to the as-received ashes. High LOI has been reported to decrease the specific gravity in sugar-cane bagasse ash (Mali and Nanthagopalan 2021) and the results in **Table 1** lend support to this finding. **Table 1** shows that RHA beneficiated through grinding for 60 minutes at a material-to-charge ratio of 1:3 satisfied the ASTM C 618 (ASTM 2019) and the BS 8615-2 (BSI 2019) minimum fineness requirement of at least 66% and 60% passing from 45 µm respectively. It may be noted that the average particle size of the R5 sample decreased significantly from 171 µm in its unbeneficiated state to 22 µm and 18 µm for grinding durations of 60 min and 100 min respectively. In the case of the R6 sample, average particle size in its beneficiated state was 25 µm compared to 228 µm in the unbeneficiated state. Similar level of fineness was obtained by (Rego et al. 2015b) using LOS Angeles test arrangement for 60 min grinding.

3.1.3.2 BET Specific Surface Area

BET Specific Surface Area (BET-SSA) of the RHAs varied in the wide range of 15 m^2/g - 50 m^2/g, **Table 1**. The higher BET-SSA in the ashes from the East (R1) and South (R2) is attributed to their higher unburnt carbon content. Since a high K_2O content is reported to decrease surface area (Bie et al. 2018), the lower surface area in R4 is attributed to its high K_2O content. Effect of grinding on BET-SSA of the control ashes (R5 and R6) may be seen with reference to **Table 1.** In the unbeneficiated control RHA samples R5 and R6, BET-SSA was 26 m^2/g and 32 m^2/g which increased to 35 m^2/g and 43 m^2/g respectively after beneficiation.

3.1.3.3 Morphology

Cellular microstructure was seen in the morphology of all the as-received ash samples, **Figure 1**, with pores being seen on the particle surface in some cases, **Figures 1 (b)** and **1 (d)**. Morphology of the beneficiated ashes is shown in **Figures 1 (g)** and **1 (h)** where agglomeration

of very fine particles with the coarser ones can be seen. Similar behaviour is also reported by (Rego et al. 2015b). Most of the macropores present on the surface of the as-received RHAs collapsed after grinding. As highlighted in **Figures 1 (g)** and **1 (h)**, surface pores continue to be present in the beneficiated ashes in spite of grinding. These fine pores on the surface are responsible for the large surface area which in turn imparts high pozzolanic reactivity.

3.1.4 Pozzolanic reactivity

According to IS 269 (BIS 2015), pozzolanic reactivity of RHA when examined in accordance with IS 1727 (BIS 1967), should be more than 90%. The 7-day and 28-day compressive strength results in **Table 1** show that none of the as-received RHA samples and the control RHA samples fulfilled this requirement. However, all the beneficiated RHA samples achieved strengths of more than 90% of the strength of the reference specimen. The increase in water demand due to the inclusion of R1 and R2 in binary binders was more than the maximum permissible limit of 115% of control in ASTM C 618 (ASTM 2019), **Table 1**. Binary binders including the beneficiated RHAs showed the least increase in water demand which was in the range of 105% - 110% of the reference. The low 28-day pozzolanic reactivity of R1 and R2 is attributed to their higher LOI (33% and 23.4% respectively) which leads to an increase in water demand for achieving the same flow as the reference sample. In **Table 1**, the high strength obtained with the beneficiated RHAs is attributed to the lower water-binder ratio and better reactivity due to the presence of fine particles as well as to the filler effect of such particles.

3.2 Standard consistency

Typical trends in standard consistency are presented in **Figure 2 (a)** which shows that the consistency of paste blended with the R5 control ash varied from 121% of that for the reference paste at 5% replacement level to 171% for 20% replacement. However, in the case of the beneficiated samples, at 5% replacement levels, consistency varied from 111% of the reference paste to 139% for 20% RHA replacement. Standard consistency of the unblended cement paste (taken as reference) was 28%. To illustrate the effect of beneficiation, the consistency of pastes blended with R5, R5-G60, and R5-G100 at 15% replacement level was 154%, 129%, and 132% of the reference paste respectively. This indicates that more water is required to maintain paste consistency with the control RHA R5 when compared to its

beneficiated counterparts R5-G60 and R5-G100. This behaviour is attributed to a breakdown in the pore structure of the RHA particles in the beneficiated samples. **Figure 2 (b)** shows that the mortar water-binder ratio calculated using the consistency of the relevant paste is higher at each replacement level of the control RHA, R5. Further, this figure also shows that at each of the replacement levels (5%, 10%, 15%, and 20%) mortars blended with the beneficiated R5 has relatively lower water demand when compared to mortars containing the unbeneficiated ash. It may be seen in **Figure 2 (b)** that increased water demand for R5 was within the allowable limit of 115% in ASTM C 618 (ASTM 2019) only as long as the cement replacement level was capped at 5% and for the beneficiated R5 this limit was 10%.

3.3 Compressive strength

Strength testing was done only with the control and the beneficiated ashes. Results of sample R5 are discussed here which are typical of the RHAs under investigation. **Figures 3 (a)** and **3 (b)** respectively present 7- and 28-day compressive strength of the reference cement mortar vis-à-vis the RHA (R5) blended cement mortar for up to 20% RHA replacement levels. These figures show that across all the RHA replacement levels, higher strengths were obtained with the beneficiated ash when compared to the control R5. Further, a decreasing trend in compressive strength of beneficiated RHA blended mortars is observed with increasing replacement levels. Compressive strength exceeding 80% of the strength of the reference mortar (with only cement as the binder) was achieved for up to 15% replacement of cement with R5-G100 at both test ages. In comparison, the compressive strength of the control RHA R5 is less than 50% of the reference mortar at 15% replacement of RHA as shown in **Figures 3 (a)** and **3 (b)**. **Figure 3 (c)** shows the compressive strength variation in the PC and the RHA (R6-G100) blended mortars investigated as per ASTM C 109 (ASTM 2020) for 110 ± 5% flow. It may be observed in this figure that to obtain flow similar to that of the PC mortar, the water-to-binder ratio increased linearly for up to 15% replacement level following which it remained constant up to 20% replacement level of RHA. A 28-day compressive strength of 95% and 92% of that of the PC mortar was achieved up to a replacement level of 15% and 20% respectively. The increase in water-binder ratio was up to 14% of that of the PC mortars prepared for 110 ± 5% flow with no significant reduction in compressive strength. This observation is similar to that made by (Chindaprasirt et al. 2007) wherein it was noted that mortar blended with 20% RHA

and containing extra water showed better compressive strength relative to the control mortar made with OPC as the only binder. The XRD analysis of mortars show the reduction in portlandite which is a crystalline phase of calcium hydroxide as shown in **Figure S2** and lower Ca/Si ratios of RHA blended mortars reported in SEM and EDS results in **Figure S3** are indicative of pozzolanic reaction of cement with RHA. Morphological properties of hydration products of lower Ca/Si ratio are supportive in the pore refinement of mortars (Rego et al. 2015a) which is in compliance with the results of mercury intrusion porosimetry tests reported on mortars in Section 3.4.

Hence, the compressive strength results obtained in the context of both the Indian and the ASTM standards indicate that the beneficiated RHA up to 15% weight replacement of cement can be used in cement mortar without any detrimental effect on 7- and 28-day compressive strength, as long as the fineness of the ash complies with the minimum requirement of ASTM C 618-19 or BS 8615-2 (BSI 2019) and amorphous silica content requirement in the IS 269: 2015 is relaxed from 80% so that in the context of this Code the beneficiated ashes also become acceptable as a pozzolan. Thus, combining the guidelines of Indian, British and ASTM Standards, RHA can be recommended for use in concrete if at least 60% particles are finer than 45 µm, SAF is > 70%, amorphous silica content is >25% and LOI of binary binder (OPC+RHA) is below 5%.

3.4 Mercury intrusion porosimetry

3.4.1 Pore Size Distribution

The relationship between pore diameter, differential pore volume, and cumulative pore volume for the plain cement mortar and the beneficiated RHA blended mortars is presented in **Figures S4 (a), (b), (c)** and **(d)** respectively. Zones with zero differential pore volume are termed as non-porous and zones showing significant differential pore volume are called porous. Both non-porous and porous zones were present in the measured range of pore diameters. Similar to results in the literature (Mangat and Ojedokun 2018), the beneficiated RHA blended mortars showed unimodal pore distribution similar to that observed in the cement mortars and peak pore volume was within the range of 0.01-0.1 µm. As shown in **Figures S4** and **4 (a)**, pore volume distribution in the RHA blended mortars tended to shift towards the lower range of pore

sizes. This behaviour is attributed to the dense microstructure achieved in the RHA mortars due to pozzolanic reactions (Wada et al. 2000).

3.4.2 Pore system parameters

The pore system parameters are derived from the cumulative and differential pore volume curves. These parameters play a significant role in assessing the microstructure of cementitious mixtures (Aligizaki 2006; Ma 2014). The representative MIP curves as shown in **Figure S4** provide information on the intrudable porosity (Φ_{in}), threshold pore diameter (d_{th}), and critical pore diameter (d_c). The average pore diameter (d_{avg}) and total porosity can be analyzed from the numerical data. The critical pore diameter corresponds to the peak intruded volume and the threshold pore diameter corresponds to the minimum continuous pore size after which there will be a sharp change in the cumulative pore volume curve. Threshold diameter was identified as the intersection of tangents of the slope changing points on the cumulative curve (Ma 2014).

3.4.2.1 Intrudable and total porosity

The volume of intrudable pores in the PC and the beneficiated RHA (R6-G100) blended mortars was determined from the cumulative pore volume curves and representative results are shown in **Figure 4 (a)** and are presented in **Table 2**. The intrudable volume was 75.42 mm^3/g for the PC mortar and was found to be more for both 15% and 20% beneficiated RHA (R6-G100) replacement though the increase was not higher than 6% of that of the PC mortar. Similarly, total porosity also increased with the addition of beneficiated RHA (R6-G100) and was in the range of 102% - 110% of that of the PC mortar. The increase in intrudable and total porosity is attributed to the higher water content used to obtain a flow in the beneficiated RHA (R6-G100) blended mortars similar to that of the PC mortar. On the other hand, (Maeda et al. 2001) report lower total porosity in RHA blended mixtures prepared using the same water-binder ratio as the control mixture. It may be observed in **Figure 4 (b)** that filled pore volume is concentrated towards the lower range of pore sizes and this parameter increases with an increase in the percentage of beneficiated RHA (R6-G100).

Pore size ranges are classified into capillary pores and gel pores (Mindess et al. 2003). Capillary pores are further divided into macropores (10-0.05 µm) and large mesopores (0.05-0.01 µm) and pores with size < 0.01µm are classified as gel pores. **Table 2** presents the percentage of pore volume filled by each of these pore sizes. Pore refinement was also noted in the higher range of particle sizes. For example, in the particle size range of >0.05 µm, the total pore volume in the PC mortar was higher when compared to mortar being prepared with 10%, 15%, and 20% beneficiated RHA (R6-G100). The experimental data in **Table 2** shows that the higher water demand associated with the use of beneficiated RHA (R6-G100) does not alter the porosity associated with macropores though the porosity associated with large mesopores increases. The lower porosity of macropores is attributed to the pore refinement due to the denser microstructure of beneficiated RHA blended mortars by pozzolanic reaction (Maeda et al., 2001). Permeability in cement mortars is directly linked with the porosity and pore sizes. According to Aligizaki (Aligizaki 2006), the mechanisms for transport processes are quite different in different categories of pores. In the case of gel pores movement of water does not contribute much to the cement paste permeability. In mesopores having sizes between 0.002 and 0.05 µm, electrostatic interactions between the pore liquid and the pore walls may hinder the transport processes but these electrostatic effects do not occur in macropores. It is therefore reckoned that despite its higher total porosity the refined pore structure in mortars blended with the beneficiated RHAs is conducive for restricting the ingress of water or other chemicals when compared to the PC mortars.

3.4.2.2 Pore diameters

The durability properties of cementitious mixtures are influenced by critical and threshold pore diameters (Ma 2014; Mangat and Ojedokun 2018). Threshold diameter can be considered as the property controlling water intrusion in mortar (Dhandapani and Santhanam 2017) and in all the mortars of this investigation the threshold diameter varies in the range 2-3 µm. **Table 2** shows that despite blending with the beneficiated RHA (R6-G100) and the associated high-water demand, no detrimental effect was observed on threshold diameters in the mortars blended with the beneficiated RHAs when compared to the PC mortars. The critical diameter for the mortar sample containing 10% beneficiated RHA was approximately similar to

that of the PC mortar however for the sample containing 15% beneficiated RHA this diameter was significantly lower than that of the PC mortar. However, for the sample containing 20% RHA, two critical pore diameters were observed, one being larger and the other being smaller than the critical size associated with the PC sample. It was also noted that the average pore diameter of each of the beneficiated RHA blended mortars was lower than the average pore diameter of the PC mortar. The reduction in both the critical and the average diameters in the beneficiated RHA (R6-G100) blended mortars is attributed to the shifting of pore size distribution towards the smaller range of pores principally due to the pore refinement by pozzolanic action of RHA. Pore refinement of cement pastes blended with RHA was also reported by (Rego et al. 2015a) which showed reduction in pore volume for the pore sizes higher than 0.05 µm.

Although total porosity in the beneficiated RHA up to 20% replacement increased as expected due to high-water dosage when compared to the PC mortar, only the large mesopores (0.05-0.01 µm) have shown an increase in pore volume percentage. Reduction in the total pore volume percentage of macropores in the beneficiated RHA blended mortars and high pore volume percentage in the finer range (0.2-0.05 µm) as shown in **Figure 4 (b)** indicates development of a dense microstructure in the blended mortars when compared to the PC mortar.

4. Conclusions

The following conclusions are drawn from the reported investigations:

a) RHA samples of unknown combustion histories and RHAs obtained from controlled combustion of husks possessed similar fineness. At least an 80% fraction of all the RHAs was coarser than 45 µm. All the RHAs had a cellular microstructure and BET-SSA was in the range of 15m^2/g – 50 m^2/g.

b) Loss on Ignition (LOI) of the as-received RHAs from the West, North, South, and the East of the country were 13%, 14%, 23%, and 33% respectively compared to 7% - 8% for both the control RHAs (R5 and R6). None of the as-received and the control RHAs satisfied the 5% upper bound LOI limit of IS: 269:2015. However, the LOI values of the control RHAs were below the maximum allowable limit of 10% for

Class-N raw or calcined natural pozzolanas given in ASTM C 618-19. Silica content in the as-received RHAs was in the range of 60%-80% whereas it was 80% - 85% for the control RHAs.

c) The R6 ash obtained from controlled burning in the temperature range of 650^{o}C-700^{o}C satisfied the 80% amorphous silica requirement of IS: 269:2015 though this was not done by the R5 ash produced at the burning temperature range of 600^{o}C-700^{o}C (70% amorphous silica content). However, both the control ashes R5 and R6 fulfilled the chemical and mineralogical requirements of ASTM C 618-19 for Class-N raw or calcined natural pozzolanas. In this context, the 80% amorphous silica requirement in IS 269: 2015 appears to be overly restrictive and will hinder ash utilisation as a supplementary cementitious material.

d) Beneficiated RHAs obtained by grinding the control ashes satisfied the minimum fineness requirements for Class-N raw or calcined natural pozzolanas given in the ASTM C 618-19 as well as for fly ash given in the IS 3812 (Part 1): 2013. The beneficiated RHAs also complied with the pozzolanic reactivity requirements of both the IS 269:2015 and the ASTM C 311-18, by achieving >90% pozzolanic reactivity. None of the as-received RHAs fulfilled this minimum pozzolanic reactivity requirement.

e) Cement pastes blended with the beneficiated RHAs had lower consistency which translates into lower water/binder ratios and higher strength. In order to obtain RHA blended mortar flow similar to that of the control cement mortar, it can be permissible to increase water content in the blended mortar to 115% of the control value. This increase has been seen to have no detrimental effect on the compressive strength of the blended mortar when compared to its control mortar.

f) Pore size distribution in the mortars blended with up to 20% replacement with the beneficiated RHAs shifted towards the lower range of pores and the volume of macropores (10-0.05 μm) in the blended mortars is less than in the PC mortar. On the other hand, the volume of large mesopores (0.05-0.01 μm) was higher in the blended mortars with no significant change in the volume of pores of size < 0.01μm.

However, the total porosity in the blended mortars was 102%-110% of the porosity of the PC mortar.

g) Threshold pore diameters in the mortars blended with the beneficiated RHA were comparable to those in the PC mortar or lower. Critical pore diameters and average pore diameters in the blended mortars were lower than those in the PC mortar for up to 15% RHA replacement.

h) Compressive strength results obtained in the context of both the relevant Indian and ASTM Standards indicate that up to 15% weight replacement of cement with the beneficiated RHAs can be used in cement mortars without any detrimental effect on the 7- and 28-day compressive strength as long as RHA fineness complies with the ASTM C 618-19 requirements and the amorphous silica content in the IS 269: 2015 is relaxed from 80% to 70% leading to the beneficiated ashes also becoming acceptable as pozzolans.

Acknowledgments

Authors acknowledge the Department of Biotechnology, New Delhi, India, to provide a research grant under the aegis of DBT-Innovate, U.K. Newton-Bhabha Fund (BT/IN/Innovate-UK/35/BS/2016-17). We are grateful to our research partners M/s Kuantum Papers Ltd. Hoshiarpur, Punjab, India to provide kind support during the performance of experiments.

The first author is grateful to the All India Council for Technical Education and Q.I.P. Centre, Indian Institute of Technology Roorkee, Roorkee, and Commonwealth Scholarship Commission, U.K. for providing a scholarship.

Disclosure Statement

No potential conflict of interest.

References

Armesto, L., Bahillo, A., Veijonen, K. et al. 2002. Combustion behaviour of rice husk in a bubbling fluidised bed. Biomass and Bioenergy 23(3): 171–179, doi: 10.1016/S0961-9534(02)00046-6.

Aligizaki, K.K., 2006. Pore Structure of Cement-Based Materials: Testing, Interpretation and Requirements, Taylor & Francis, Abingdon, England.

ASTM 2018. Standard Test Methods for Sampling and Testing Fly Ash or Natural Pozzolans for Use in Portland-Cement Concrete. United States: American Standard Test Method. ASTM C 311-18.

ASTM 2019. Standard Specification for Coal Fly Ash and Raw or Calcined Natural Pozzolan for Use in Concrete. United States: American Standard Test Method. ASTM C 618-19.

ASTM 2020. Standard Test Methods for Compressive Strength of Hydraulic Cement Mortars. United States: American Standard Test Method. ASTM C109-20.

BIS 2015. Ordinary Portland Cement – Specification. New Delhi: Bureau of Indian Standards. IS: 269:2015.

BIS 1991. Standard Sand for Testing Cement- Specification. New Delhi: Bureau of Indian Standards. IS: 650:1991 (Reaffirmed 2018).

BSI 2019. Specification for pozzolanic materials for use with Portland cement. BSI Standards Publication. BS 8615-2.

BIS 1967. Methods of Test for Pozzolanic Materials. New Delhi: Bureau of Indian Standards. IS: 1727:1967 (Reaffirmed 2018).

BIS 1988. Methods of Physical Tests for Hydraulic Cement-Determination of consistency of standard cement paste. New Delhi: Bureau of Indian Standards.IS: 4031(Part-4):1988 (Reaffirmed 2019).

BIS 1988. Methods of Physical Tests for Hydraulic Cement-Determination of Compressive Strength of Hydraulic Methods of Physical Tests for Hydraulic Cement. New Delhi: Bureau of Indian Standards. IS: 4031(Part-6):1988 (Reaffirmed 2019).

BIS 2013. Pulverized Fuel Ash-Specification. New Delhi: Bureau of Indian Standards. IS: 3812:2013 (Part-1) (Reaffirmed 2017).

Blissett, R., Sommerville, R., Rowson, N. et al. 2017. Valorisation of rice husks using a TORBED® combustion process. Fuel Processing Technology 159: 247–255, doi: 10.1016/j.fuproc.2017.01.046.

Bie, R., Song, X., Liu, Q. Ji. et al. 2018. Studies on effects of burning conditions and rice husk ash (RHA) blending amount on the mechanical behavior of cement. Cement and Concrete Composites 55: 162–168, doi: 10.1016/j.cemconcomp.2014.09.008.

551 Batra, V.S., Urbonaite, S., and Svensson, G. 2008. Characterization of unburned carbon in
552 bagasse fly ash. Fuel 87(13–14): 2972–2976, doi: 10.1016/j.fuel.2008.04.010.
553 Chen, G., Du, G., Ma, W. et al. 2015. Production of amorphous rice husk ash in a 500 kW
554 fluidized bed combustor. Fuel 144 :214–221, doi: 10.1016/j.fuel.2014.12.012.
555 Chandrasekhar, S., Pramada, P.N., and Majeed, J. 2006. Effect of calcination temperature and
556 heating rate on the optical properties and reactivity of rice husk ash. Journal of Materials
557 Science 41(23) : 7926–7933, doi: 10.1007/s10853-006-0859-0.
558 Chindaprasirt, P., et al. 2007. Sulfate resistance of blended cements containing fly ash and rice
559 husk ash. Construction and Building Materials 21(6): 1356–1361. doi:
560 10.1016/j.conbuildmat.2005.10.005.
561 Dizaji, H.B., Zeng, T., Hartmann, I. 2019. Generation of High Quality Biogenic Silica by
562 Combustion of Rice Husk and Rice Straw Combined with Pre- and Post-Treatment
563 Strategies — A Review. Applied Sciences 9 :1–27, doi: 10.3390/app9061083.
564 Dhandapani, Y., and Santhanam, M. 2017. Assessment of pore structure evolution in the
565 limestone calcined clay cementitious system and its implications for performance. Cement
566 and Concrete Composites 84: 36–47, doi: 10.1016/j.cemconcomp.2017.08.012.
567 Fernandes, I.J., Calheiro, D., Kieling, A.G. et al. 2016. Characterization of rice husk ash
568 produced using different biomass combustion techniques for energy. Fuel 165: 351–359,
569 doi: 10.1016/j.fuel.2015.10.086.
570 FAO 2018. FAO Rice Market Monitor. Food and Agriculture Organization of the United States,
571 21(1), pp. 1–38.
572 Ganesan, K., Rajagopal, K., and Thangavel, K. 2008. Rice husk ash blended cement:
573 Assessment of optimal level of replacement for strength and permeability properties of
574 concrete. Construction and Building Materials 22:1675–1683.
575 Gastaldini, A.L.G., Isaia, G.C., Hoppe, T.F. et al. 2009. Influence of the use of rice husk ash on
576 the electrical resistivity of concrete: A technical and economic feasibility study. Construction
577 and Building Materials 23: 3411–3419.
578 Huang, H., Gao, X., Wang, H. et al. 2017. Influence of rice husk ash on strength and
579 permeability of ultra-high performance concrete. Construction and Building Materials
580 149:621–628.

581 Maeda, N., Wada, I., Kawakami, M. et al. 2001. Chloride Diffusivity of Concrete Incorporating
582 Rice Husk Ash. ACI Special Publication 200: 291–308.
583 Mangat, P.S., and Ojedokun, O.O. 2018. Influence of curing on pore properties and strength of
584 alkali activated mortars. Construction and Building Materials 188:337–348.
585 Mali, A.K., and Nanthagopalan, P. 2021. Thermo-mechanical treatment of sugarcane bagasse
586 ash with very high LOI : A pozzolanic paradigm. Construction and Building Materials (in
587 press) 288 :122988, doi: 10.1016/j.conbuildmat.2021.122988.
588 Ma, H. 2014. Mercury intrusion porosimetry in concrete technology: Tips in measurement, pore
589 structure parameter acquisition and application. Journal of Porous Materials 21:207–215.
590 Mindess, D.S., Young, J.F., and Darwin 2003. Concrete, Prentice-Hall, Pearson Education, Inc.,
591 Upper Saddle River, N.J. 07458, U.S.A.
592 Nehdi, M., Duquette, J., and El Damatty, A. 2003. Performance of rice husk ash produced using
593 a new technology as a mineral admixture in concrete. Cement and Concrete Research 33(8)
594 : 1203–1210, doi: 10.1016/S0008-8846(03)00038-3.
595 Nair, D.G., Jagadish, K.S., and Fraaij, A. 2006. Reactive pozzolanas from rice husk ash: An
596 alternative to cement for rural housing. Cement and Concrete Research 36(6): 1062–1071,
597 doi: 10.1016/j.cemconres.2006.03.012.
598 Olalekan, O., and Mangat, P.S. 2018. Characterization and Pore Structure of Rice Husk Ash
599 Cementitious Materials. ACI Special Publication: Durability and sustainability of concrete
600 structures 326: 8.1-8.10.
601 Rozainee, M., Ngo, S.P., Salema, A.A. et al. 2008. Fluidized bed combustion of rice husk to
602 produce amorphous siliceous ash. Energy for Sustainable Development 12(1): 33–42, doi:
603 10.1016/S0973-0826(08)60417-2.
604 Rêgo, J.H.S., Nepomuceno, A.A., Figueiredo, E.P. et al. 2015a. Microstructure of cement
605 pastes with residual rice husk ash of low amorphous silica content. Construction and
606 Building Materials 80:56–68, doi: 10.1016/j.conbuildmat.2014.12.059.
607 Rêgo, J.H.S. et al. 2015b. Effect of Particle Size of Residual Rice-Husk Ash in Consumption of
608 $Ca(OH)_2$. Journal of Materials in Civil Engineering 27(6): 04014178, doi:
609 10.1061/(asce)mt.1943-5533.0001136.

610 Singh, B. 2018. Rice husk ash. Waste and Supplementary Cementitious Materials in Concrete:
611 Characterisation, Properties and Applications, Elsevier. pp. 417-460, doi: 10.1016/B978-0-
612 08-102156-9.00013-4.
613 Singh, A., and Singh, B. 2020. Characterization of rice husk ash obtained from an industrial
614 source. Journal of Sustainable Cement-Based Materials 10(4): 193-212, doi:
615 10.1080/21650373.2020.1789010.
616 Van, V.T.A., Rößler, C., Bui. D.D. et al. 2013. Mesoporous structure and pozzolanic reactivity of
617 rice husk ash in cementitious system. Construction and Building Materials 43: 208–216, doi:
618 10.1016/j.conbuildmat.2013.02.004.
619 Venkatanarayanan, H.K., and Rangaraju, P.R. 2013. Material Characterization Studies on Low-
620 and High-Carbon Rice Husk Ash and Their Performance in Portland Cement Mixtures.
621 Advances in Civil Engineering Materials 2 : 20120056.
622 Wada, I., Kawano, T., Kawakami, M. et al. 2000. Effect of Highly Reactive Rice Husk Ash on
623 Durability of Concrete and Mortar. ACI Special Publication 192:205–222.
624 Xu, W., Lo, T.Y., and Memon, S.A. 2012. Microstructure and reactivity of rich husk ash.
625 Construction and Building Materials 29: 541–547, doi: 10.1016/j.conbuildmat.2011.11.005.
626 Zunino, F., and Lopez, M. 2017. A methodology for assessing the chemical and physical
627 potential of industrially sourced rice husk ash on strength development and early-age
628 hydration of cement paste. Construction and Building Materials 149: 869–881, doi:
629 10.1016/j.conbuildmat.2017.05.187.
630 Zain, M.F.M., Islam, M.N., Mahmud, F. et al. 2011. Production of rice husk ash for use in
631 concrete as a supplementary cementitious material. Construction and Building Materials
632 25(2) : 798–805, doi: 10.1016/j.conbuildmat.2010.07.003.
633
634 **List of Figure Legends:**

635 Figure 1. SEM images of the all RHAs (1000x) (a) R1 (b) R2 (c) R3 (d) R4 (e) R5 (f) R6 g) R5-
636 G100 (2000x) and h) R6-G100 (2000x).

637 Figure 2. Cement replacement versus a) Consistency of control and beneficiated RHA, R5
638 blended pastes b) Water-binder ratio of mortars associated with consistency of pastes.

Figure 3. Compressive strength versus cement replacement for the control and beneficiated RHA blended mortars as per IS 4031 (Part 6) (BIS, 1988) at (a) 7-day (b) 28-day and (c) as per ASTM C 109 (ASTM, 2020) at 7- and 28-day.

Figure 4. a) Cumulative Pore volume distribution of the PC and RHA blended mortars, and b) Relationship between pore volume and incremental pore diameter range.

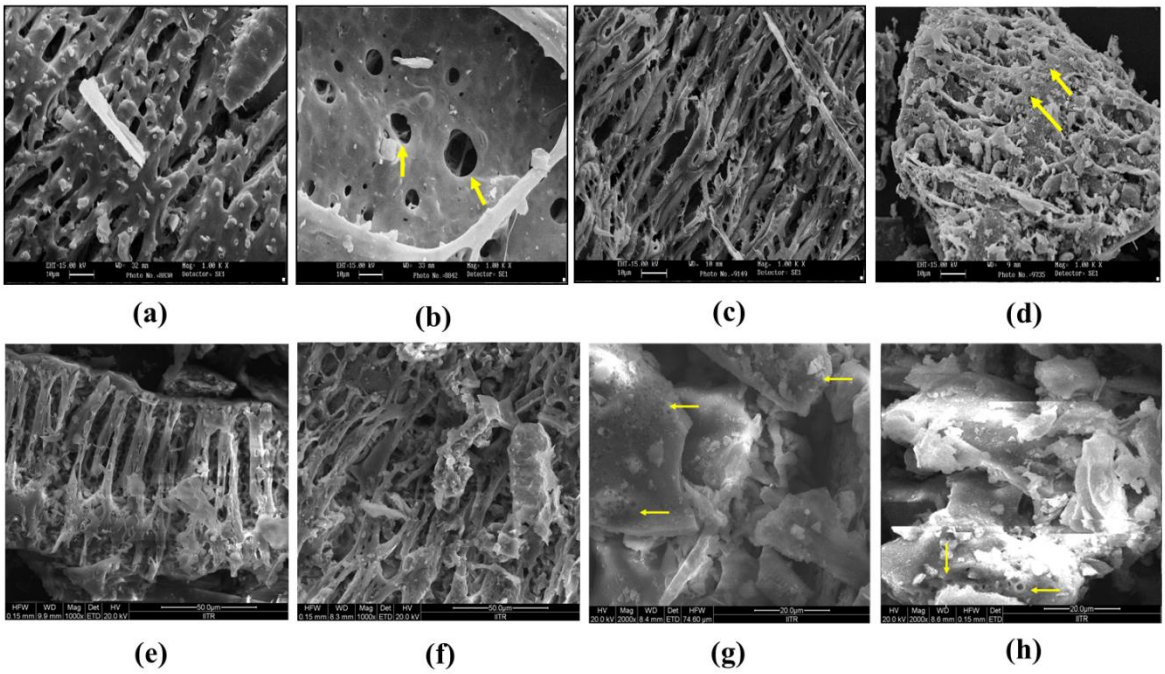

Figure 1: SEM images of the all RHAs (1000x) (a) R1 (b) R2 (c) R3 (d) R4 (e) R5 (f) R6 g) R5-G100 (2000x) and h) R6-G100 (2000x).

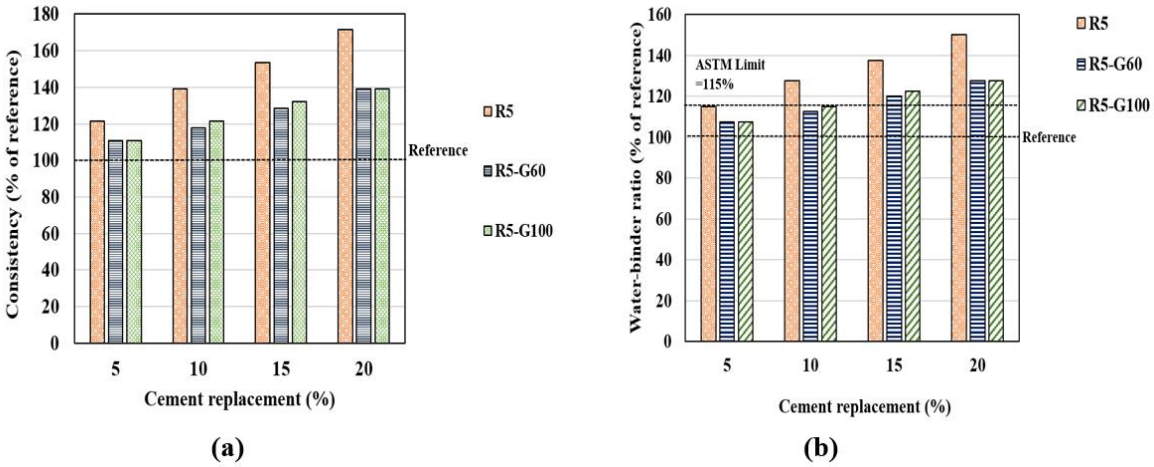

650
651
652 **Figure 2: Cement replacement versus a) Consistency of control and beneficiated RHA,**
653 **R5 blended pastes b) Water-binder ratio of mortars associated with consistency of**
654 **pastes.**

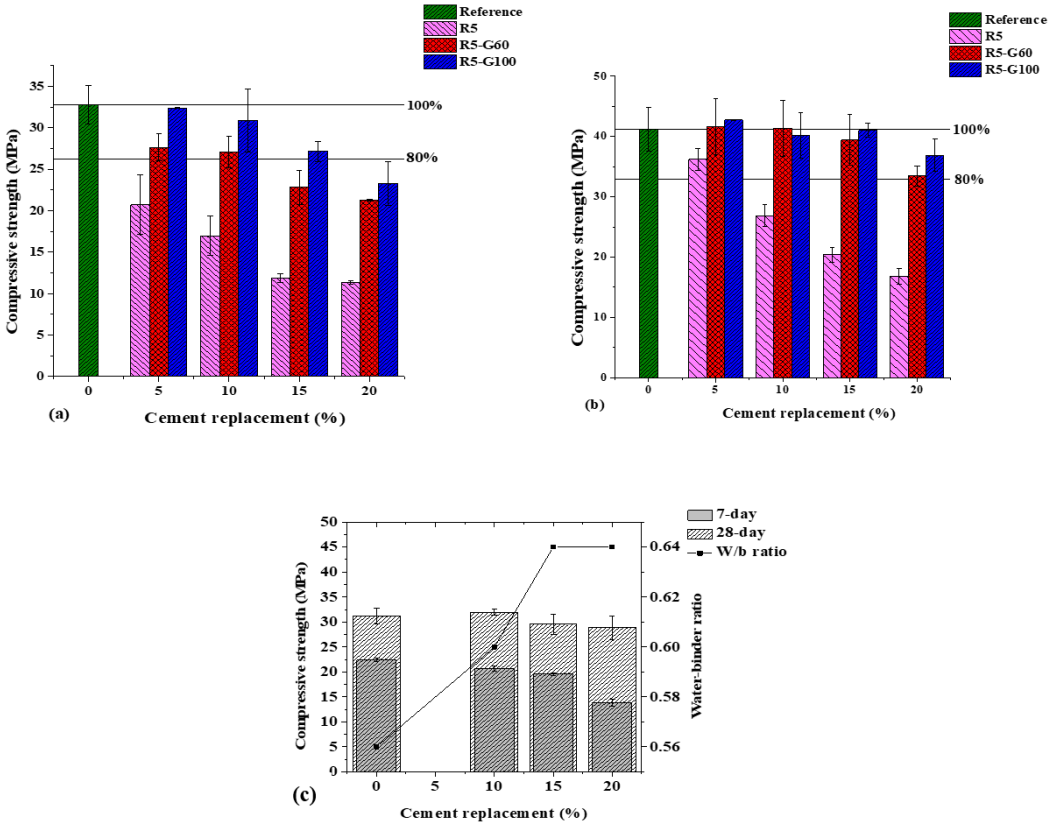

655
656 **Figure 3: Compressive strength versus cement replacement for the control and**
657 **beneficiated RHA blended mortars as per IS 4031 (Part 6) (BIS, 1988) at (a) 7-day (b) 28-**
658 **day and (c) as per ASTM C 109 (ASTM, 2020) at 7- and 28-day.**
659

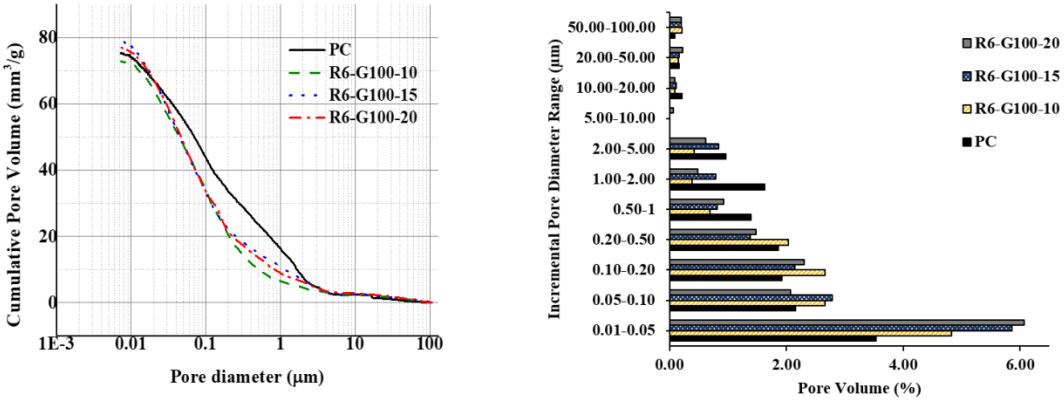

(a) (b)

Figure 4: a) Cumulative Pore volume distribution of the PC and RHA blended mortars, and b) Relationship between pore volume and incremental pore diameter range.

Table 1. Properties of the as-received, control and beneficiated RHA samples.

	R1	R2	R3	R4	R5	R6	R5-G60	R5-G100	R6-G100
Chemical composition (%)									
Na_2O	0.11	0.13	0.75	0.29	0.83	0.49	-	-	-
MgO	0.28	0.33	0.56	0.64	0.90	0.71	-	-	-
Al_2O_3	0.10	0.11	0.59	2.57	2.28	1.58	-	-	-
SiO_2	61.3	70	80	72.2	80.2	84.4	-	-	-
P_2O_5	1.1	1.24	0.83	0.62	0.65	0.46	-	-	-
SO_3	0.45	0.52	0.66	0.21	0.31	0.15	-	-	-
K_2O	2.2	2.56	1.60	6.12	4.07	3.07	-	-	-
CaO	0.49	0.55	0.97	1.26	1.16	0.63	-	-	-
TiO_2	-	-	-	-	0.09	0.08	-	-	-
MnO	0.15	0.17	0.08	0.07	0.15	-	-	-	-
Fe_2O_3	0.4	0.45	0.41	1.49	1.1	0.71	-	-	-
Cl	0.32	0.37	0.55	0.98	0.42	0.35	-	-	-
LOI* (%)	33	23.4	13	14	7.7	7.3	-	-	-
Amorphous SiO_2 (%)	61.3	70	75	64	70	80	-	-	-
Total Amorphous (%)	100	100	95	92	90	95	-	-	-
Wet Sieve Analysis (% passing)									
75 µm	11	25	20.4	10	12.1	10.5	77.9	82.9	83.08
45 µm	8.5	20	8.9	2.5	7.4	7.2	66.6	70.4	71.4
BET-SSA (m^2/g)	49	42	32	15	26	32	32	35	43
Specific Gravity	1.63	1.7	1.8	1.9	2.15	2.10	2.19	2.2	2.16
Average Particle Size, d_{50} (µm)	-	-	-	-	171	228	22	18	25
Pozzolanic reactivity (%)									
7-day	43.81	57.78	69.72	67.19	76.70	73.81	86.40	93.60	99.97
28-day	52.33	62.81	79.21	75.10	84.50	85.98	94.70	96.20	97.88
Water requirement (% of reference)	120	118	114	114	113	113	109	107	107

*LOI: Loss On Ignition

Table 2: Pore system parameters for the PC and RHA blended mortars.

Mix	Porosity		Pore Diameters (μm)			Pore Volumes (%)		
						Pore Diameter Range (μm)		
	Intrudable (mm^3/g)	Porosity (%)	Threshold (d_{th})	Critical (d_c)	Average (d_{avg})	<0.01	0.01 - 0.05	>0.05
PC	75.42	13.92	3.012	0.0898	0.057	0.27	3.47	10.18
R6-G100-10	72.80	14.30	2.000	0.1000	0.048	0.15	4.83	9.32
R6-G100-15	79.34	15.11	3.009	0.0311	0.042	0.36	5.72	9.03
R6-G100-20	76.99	14.55	2.003	0.1593/ 0.0480	0.046	0.25	5.19	9.11

Supplementary material

Table S1: Identification of the RHA samples.

No.	Sample	Nomenclature	Source	Combustion Technique	Combustion Temperature	Region	Grinding Time (mins.)
1	As-received	R1	Gosai Rice Mills, Bijabahal, Odisha.	Unknown	Unknown	East	-
2		R2	Jai Bhawani Agencies, Gulbarga, Karnataka.	Unknown	Unknown	South	-
3		R3	Hari Om Traders, Junagadh, Gujrat.	Unknown	Unknown	West	-
4		R4	Kuantum Papers, Hoshiarpur, Punjab.	Fluidised Bed	Unknown	North	-
5	Control	R5	Kuantum Papers, Hoshiarpur, Punjab.	Fluidised Bed	600^{o}C-700^{o}C	North	-
6		R6	Kuantum Papers, Hoshiarpur, Punjab.	Fluidised Bed	650^{o}C -700^{o}C	North	-
7	Beneficiated	R5-G60	-do-	-do-			60
8		R5-G100					100
9		R6-G100					100

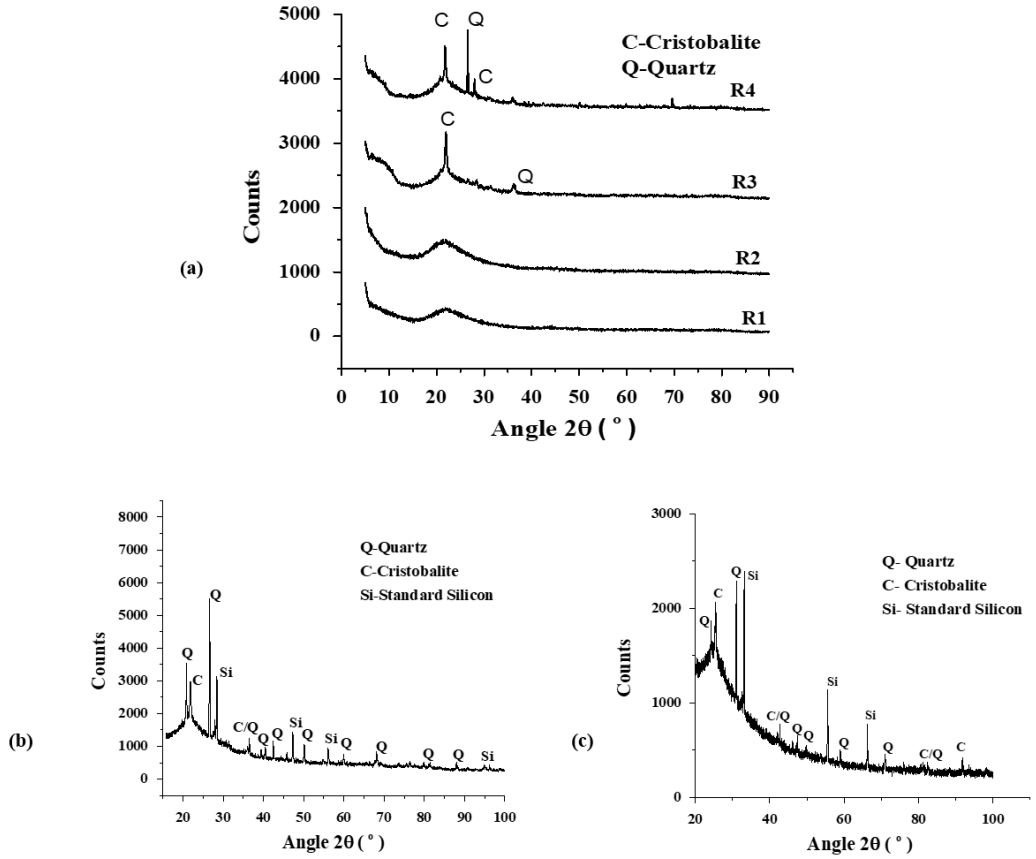

Figure S1: X-ray diffractogram of (a) R1, R2, R3, R4 (b) R5 and (c) R6.

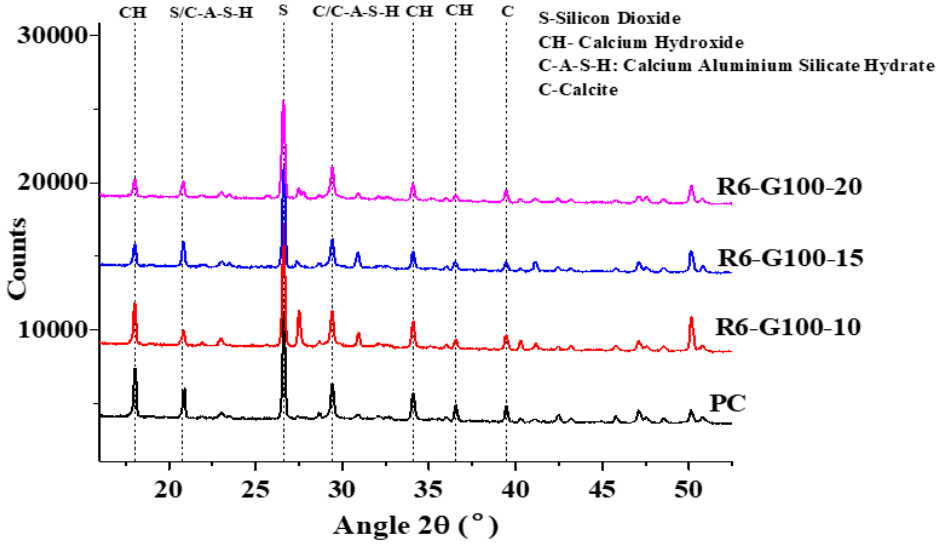

Figure S2: XRD patterns for the PC and the blended mortars after curing for 28-days.

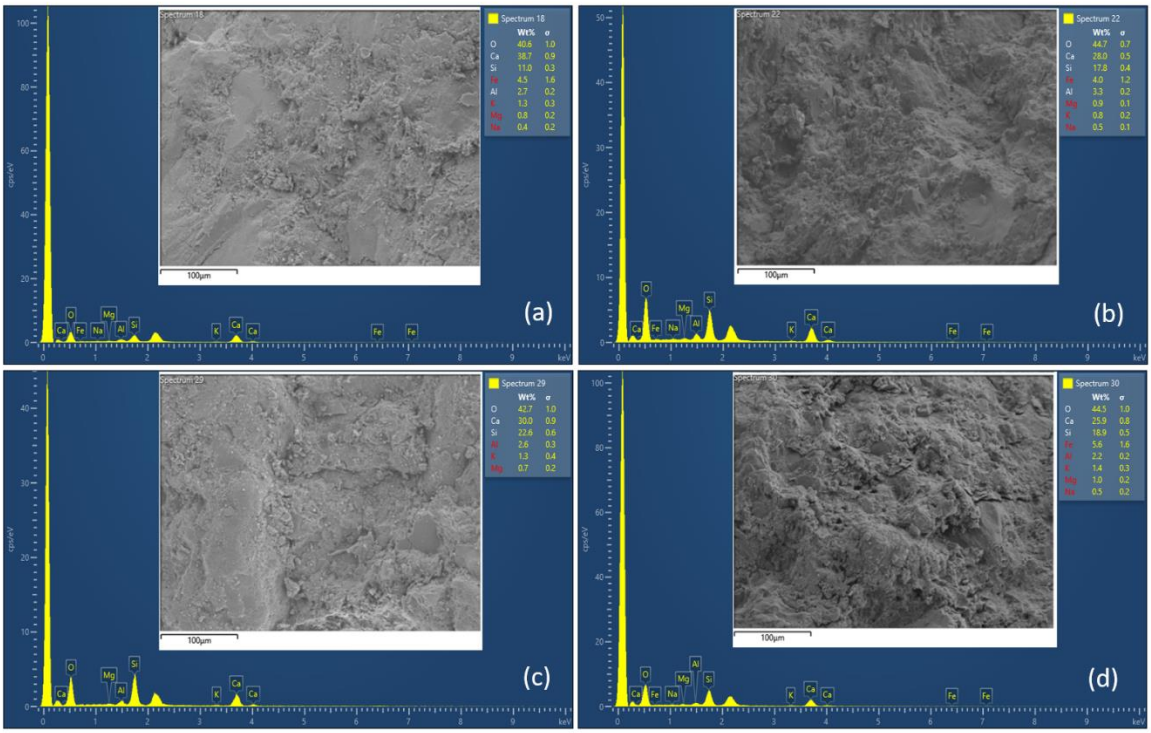

Figure S3: SEM and EDX of mortars at 28-days a) PC b) R6-G100-10 c) R6-G100-15 and d) R6-G100-20

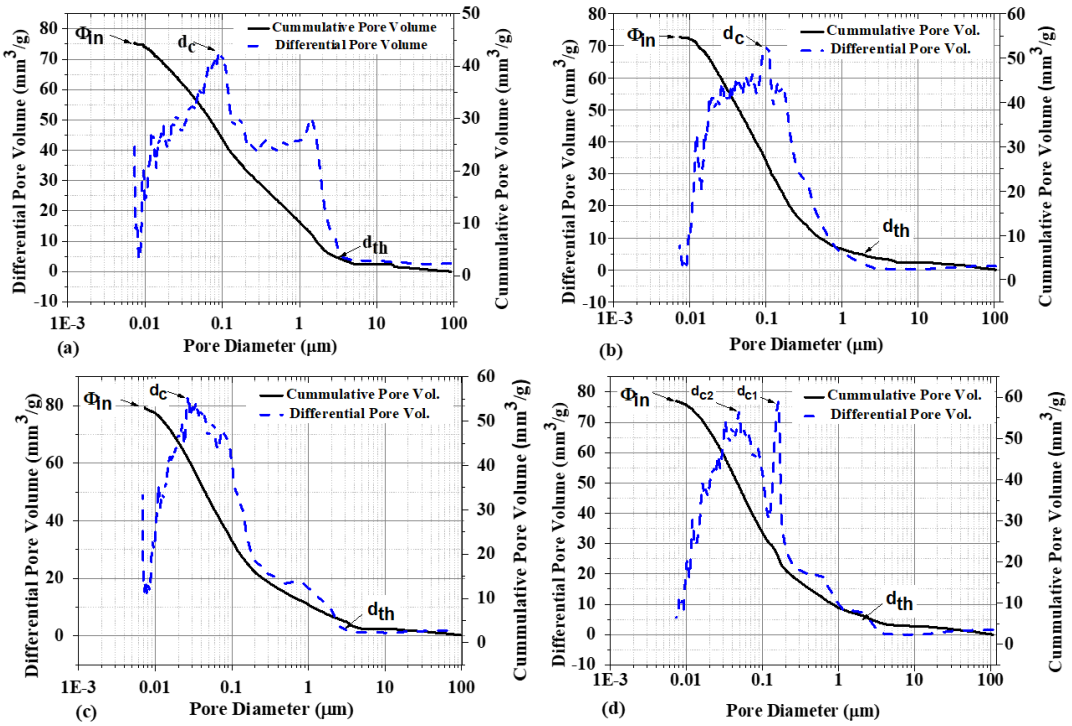

Figure S4: Pore size distribution for mortars a) PC b) R6-G100-10 c) R6-G100-15 and d) R6-G100-20